

Unreliability Tracing of Power Systems with Reservoir Hydropower Based on a Temporal Recursive Model

Yunjie Bai¹, Kaigui Xie¹, changzheng Shao¹, and Bo Hu¹

¹Chongqing University

April 03, 2024

Abstract

Power system unreliability tracing model allocates the system's reliability index to individual components, identifying potential weaknesses. This study expands its scope by considering the impact of storage resources. Unreliable factors leading to load shedding are categorized into two groups: objective factors inherent to the component and insufficient storage resources. The latter requires a retrospective analysis of other components that caused unreliability previously. When allocating responsibility for load shedding at a certain time, it begins by allocating it among components based on differences between fixed expected output and actual supply. Expected output insufficiency is considered the unreliable factor. This insufficiency due to insufficient storage resources is then decomposed into segments, each caused by excessive output in earlier instances of the same component. The expected output excess is attributed to the expected output insufficiency of other components in previous times, for which responsibility has been allocated to each component. Consequently, the expected output insufficiency at a particular time can be traced back based on a temporal recursive model, with the load shedding further allocated to components before that time. Case studies based on several systems demonstrate that the proposed model's allocation results are reasonable and more accurate than the traditional model.

Hosted file

IET-20240131-Unreliability Tracing of Power Systems with Reservoir Hydropower Based on a Temporal Recursive Model is available at <https://authorea.com/users/761595/articles/737749-unreliability-tracing-of-power-systems-with-reservoir-hydropower-based-on-a-temporal-recursive-model>

Unreliability Tracing of Power Systems with Reservoir Hydropower Based on a Temporal Recursive Model

Yunjie Bai¹, Kaigui Xie^{1*}, Changzheng Shao¹, Bo Hu¹

¹ State Key Laboratory of Power Transmission Equipment & System Security and New Technology, Chongqing University, Chongqing 400044, China

* [E-mail: kaiguixie@vip.163.com](mailto:kaiguixie@vip.163.com)

Abstract: Power system unreliability tracing model allocates the system's reliability index to individual components, identifying potential weaknesses. This study expands its scope by considering the impact of storage resources. Unreliable factors leading to load shedding are categorized into two groups: objective factors inherent to the component and insufficient storage resources. The latter requires a retrospective analysis of other components that caused unreliability previously. When allocating responsibility for load shedding at a certain time, it begins by allocating it among components based on differences between fixed expected output and actual supply. Expected output insufficiency is considered the unreliable factor. This insufficiency due to insufficient storage resources is then decomposed into segments, each caused by excessive output in earlier instances of the same component. The expected output excess is attributed to the expected output insufficiency of other components in previous times, for which responsibility has been allocated to each component. Consequently, the expected output insufficiency at a particular time can be traced back based on a temporal recursive model, with the load shedding further allocated to components before that time. Case studies based on several systems demonstrate that the proposed model's allocation results are reasonable and more accurate than the traditional model.

1. INTRODUCTION

High proportion of wind power has become the focus of global attention[1–3]. However, load-shedding due to the fluctuation and intermittence of wind power is on the rise[4–6], with the massive integration of wind power into the power systems. Hydropower stations with a reservoir can start and respond quickly to wind change and can act as a storage facility to store water during periods of high wind power output[7, 8]. Moreover, hydropower is a renewable energy with mature technology and reliability. It is the third largest power source after coal and natural gas, accounting for 15% of global electricity generation[9]. By 2022, the global hydropower installed capacity reaches 1392GW[1]. Therefore, wind power and hydropower not only account for a large proportion of the installed capacity in power systems, but also their coordinated operation can promote the consumption of new energy while ensuring system reliability[7, 10–12]. Weak components identification of such systems can help electricity companies devote limited resources and time to the most critical components in guiding power system planning and operation[13–16].

Several methods have been proposed to identify weak components[17], such as the sensitivity analysis method[18, 19], and the unreliability tracing method[20, 21]. The unreliability tracing method can allocate the power system reliability index to each component after only one reliability evaluation calculation. Thus, the degree of each component's unreliable "responsibility" is known, the identification of the weak components can be explicit and unambiguous, and remedial measures can be taken easily. The existing unreliability tracing models mainly include two categories. One category is aimed at traditional power systems taking thermal units as the main energy supply[20]. This type of model can be summarized as two principles: The failure component sharing principle (FCSP) and the proportional sharing principle (PSP). The other category is aimed at power systems with high penetration of wind power[21].

Reference [21] regards the fluctuation of wind power output as the first-order derivative of power output with respect to time, while the power output shortage caused by unit failure is the zero-order derivative of power output with respect to time. And through two decompositions, the load shedding at a certain time is decomposed into three parts according to the occurrence time of unreliable factors. The first part of load shedding is due to the remaining unreliable factors that happened before the last time, the second part is due to the shortage of system ramping capacity even if no units fail between the last time and the certain time, and the third part is due to the thermal unit failure and wind power fluctuation between the last time and the certain time. At the same time, the first-order derivative of the power output, that is, the expected ramping output, is used as the smallest unit to quantify the load shedding responsibility. Finally, reference [21] develops the first type of model, which can realize the unified allocation the responsibility for the two types of unreliable factors, namely 1st order and 0th order. These factors include wind power fluctuation, wind power intermittence, and unit failures.

However, a hydropower station equipped with a reservoir may face electricity generation limitations when the reservoir's water is insufficient. Compared with unit failure and insufficient wind power output, this type of unreliable factor at a certain time may be caused by other unreliable factors in previous times. This is because the output of a hydropower station equipped with a reservoir is controllable. When there are unreliable factors before and the system may shed load, the scheduling will increase the output of the hydropower station at that time. This will lead to a reduction in the water volume of the hydropower station. The multiple occurrences of this type of process will result in the accumulation of reductions in water volume. Compared with thermal power, which also has controllable and consumable primary energy, the primary energy of thermal power is abundant, while the primary energy of hydropower stations is limited. The mathematical integration of other unreliable factors in the past can result in the overconsumption and

depletion of water volume. Consequently, this may lead to insufficient power generation capacity in hydropower stations. Therefore, when the load shedding at a certain time is caused by the water resources of a hydropower station being overconsumed, the responsibility needs to be borne by the unreliable factors in the previous times.

To trace the responsibility of past unreliable factors, it is necessary to compile data on the historical surplus output of the hydropower station at each instance and the corresponding deficits in other components. However, there may be cases where the deficiency in a particular component during past instances is also attributable to other unreliable factors. If the responsibility is allocated by modifying the expected value of each component at that moment through the cumulative information of the previous sequence, multiple and indeterminate numbers of nested loops may be required.

Therefore, this paper allocates the responsibility of the load shedding based on a temporal recursive model. Firstly, the load shedding at a certain time is allocated among each component based on their respective differences between the fixed expected output and the actual supply at that time. Subsequently, the expected output insufficiency of a certain component due to insufficient storage resources is decomposed into multiple segments, each segment's output insufficiency being caused by excessive output in earlier instances of the same component. The expected output excess of that specific component is due to the expected output insufficiency of other components in the previous times, for which responsibility has been allocated to each component. Therefore, the expected output insufficiency at a particular time can be traced back based on a temporal recursive model, with the load shedding further allocated to components before that time.

In addition, in power systems with wind power, load shedding due to the fluctuation of wind power is on the rise. When uniformly allocating the responsibility for load shedding caused by many types of unreliable factors, including wind power fluctuation, wind power intermittence, unit failures, and insufficient water storage, it is necessary to use expected ramping as the smallest unit for quantifying responsibility[21]. In the above recursive model, the decomposition process of the expected output insufficiency is also the decomposition of the over-consumed water resources. The water volume is the double integral of the ramping versus time. However, the single-time sequence decomposition of the over-consumed water resources can only achieve the first-order differential, and it cannot allocate the load shedding to each component based on the expected ramping output. In this regard, this paper decomposes the over-consumption of water resources twice in a time series. And the overconsumption of water resources is eventually traced back to the previous expected ramping insufficiency of other components and the previous load shedding, for which responsibility has been allocated to each component.

To sum up, this paper develops the existing model, which can realize the unified quantitative allocation of load shedding, considering wind power fluctuation, wind power intermittence, unit failures, and insufficient water storage. Several systems are used to validate the rationality of the model.

2. CLASSIFICATION OF UNRELIABLE FACTORS

The power output of the generation needs to follow the change of the load, to achieve the real-time power balance. That is, the chronological power output curve $P(t)$ needs to follow the chronological load curve $L(t)$, where t is the time. $L(t)$ is expected to be borne by all system components, including wind power, thermal power, and hydropower. There will be no load shedding when all components meet their expected power output.

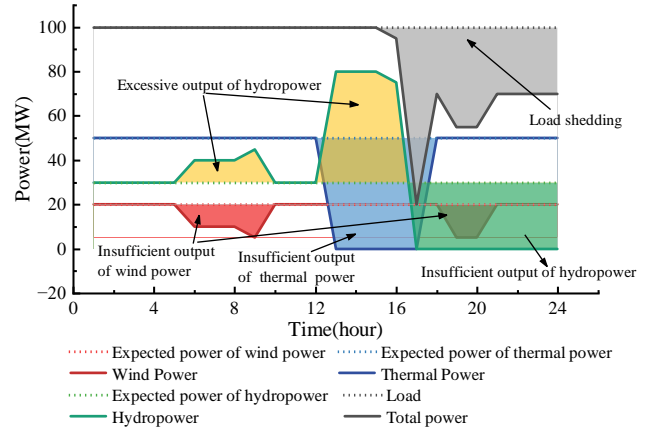


Figure 1 Load shedding scenario for power systems with hydropower

However, as shown in the gray area of Figure 1, load shedding occurs when the power of the components is insufficient, i.e., lower than the expected value. The unreliable factors contributing to this insufficient power during this period are classified into two categories:"

Category 1): The objective factor of the component itself

The insufficient output of wind power in the red area of Figure 1 due to the intermittence of wind power, and the insufficient output of thermal power in the blue area of Figure 1 due to the failure of thermal power units are all such factors. Of course, if the failure of the hydropower units leads to insufficient output of hydropower, it also belongs to this category of factors.

Category 2): The insufficient storage resources of the component

The insufficient output of hydropower in the green area of Figure 1 due to the insufficient storage of water belongs to this category of factor. The insufficient storage of water is caused by the excessive output of hydropower in the yellow area in the pre-sequence period. And the excessive output of hydropower in the yellow area in the pre-sequence periods is due to the insufficient output of wind power in the red area and the insufficient output of thermal power in the blue area. In these periods, the insufficient output of wind power and thermal power may cause the system to lose load. In order to reduce the lost load, the scheduling subjectively makes the hydropower increase output more than the expected value. That is, the second type of unreliable factors is caused by controllable, consumable, and limited resources, being cumulatively overconsumed in advance, through subjective scheduling strategies when the system may shed load due to other unreliable factors in the pre-sequence period.

Therefore, for Category 1) unreliable factors, the responsibility is allocated to the component itself. While for Category 2) unreliable factors caused by insufficient storage resources, it is necessary to trace back the components that caused unreliable factors in the pre-sequence period based on a retrospective allocation model.

Meanwhile, in power systems with wind power, reliability assessment needs to consider not only the unit's capacity constraints and water storage constraints but also the unit's ramping constraints. And when allocating the responsibility for load shedding, in addition to unreliable factors such as wind power intermittence, unit failures, and insufficient water storage, wind power fluctuation also needs to bear responsibility. The latter belongs to the first-order derivative of the power output with respect to time [21]. Therefore, it is necessary to decompose the load shedding and use the expected ramp as the smallest unit to quantify the responsibility [21]. In this situation, the power output curve and load curve are generally linear models, expressed as:

$$P(t) = P(t-1) + \Delta t \times P'(t-1) \quad (1)$$

$$L(t) = L(t-1) + \Delta t \times L'(t-1) \quad (2)$$

Where Δt is the time interval scale between time t and time $t-1$. $P'(t-1)$ is the first derivative of $P(t-1)$, and $L'(t-1)$ is the first derivative of $L(t-1)$. Subtract formula (1) and formula (2) to get:

$$E(t) = E(t-1) + R_D(t) - R(t) \quad (3)$$

Where $E(t)=L(t)-P(t)$, $E(t-1)=L(t-1)-P(t-1)$, $R_D(t)=\Delta t \times L'(t-1)$, $R(t)=\Delta t \times P'(t-1)$. $E(t)$ and $E(t-1)$ are the load shedding at time t and time $t-1$ respectively. $R_D(t)$ is the ramping demand in period $(t-1,t)$, and $R(t)$ is the actual ramping supply in period $(t-1,t)$. For the sake of simplicity, the subsequent time t is marked on the upper right of the variable.

The expected ramping of each component is defined as $R'_{K,D}$, $K=1,2,\dots,n$, which is predetermined by pre-scheduling, and their sum is R'_D . K is the serial number of component, and n is the total number of components. Certainly, the greater the capacity of the component, the greater the expected responsibility, and the system's expectation for a wind farm is often that the power output does not drop. Correspondingly, the actual ramping supply of each component is R'_K . Since all components endeavor to meet their respective expected ramping, this paper analyzes the factors that affect the maximum ramping supply for thermal units and hydropower stations. The maximum ramping supply of thermal unit K in period $(t-1,t)$ is denoted by formula (4). The maximum ramping supply of hydropower station reservoir K in period $(t-1,t)$ is denoted by formula (5), without considering other reservoir constraints. The ramping supply of wind farm K in period $(t-1,t)$ is denoted by formula (6). Then, the load shedding at time t can also be expressed as formula (7), which takes into account the fluctuation of wind power, the ramping constraints of the unit, the storage capacity constraints of hydropower, and unit failure.

$$R'_{K,N} = \min(P_K^{t-1} + r_K \Delta t, P_{K,max}) \times S_K^t - P_K^{t-1}, K \in \Phi \quad (4)$$

$$R'_{K,N} = \min\left(\left(V_K^{t-1} + I_K^t - V_{K,min}\right) A_K H_K / \Delta t - P_K^{t-1}, P_{K,max} \times S_K^t - P_K^{t-1}\right), K \in \Psi \quad (5)$$

$$R'_K = P'_K - P_K^{t-1}, K \in \Omega \quad (6)$$

$$E^t = \max\left(0, E^{t-1} + R'_D - \sum_{K \in (\Phi \cup \Psi)} R'_{K,N} - \sum_{K \in \Omega} R'_K\right) \quad (7)$$

Where Φ , Ψ , and Ω are the set of thermal units, hydropower stations, and wind farms respectively; r_K is the rated ramp rate of component K ; $P_{K,max}$ is the rated power-capacity of component K ; P_K^{t-1} is the actual power supply of component K at time $t-1$; S_K^t is the state of component K in period $(t-1,t)$, $S_K^t=1$ denotes the normal state, and $S_K^t=0$

denotes the fault state; V_K^{t-1} is the actual water volume of reservoir K at time $t-1$; I_K^t is the volume of natural inflow in period $(t-1,t)$; $V_{K,min}$ is the minimum water volume of reservoir K ; A_K is the generation efficiency of reservoir K ; H_K is the hydropower head of reservoir K . Since the water resources of the hydropower reservoir are shared by multiple hydropower units in the hydropower station, the whole hydropower station including multiple units in one reservoir is taken as a single responsible component when allocating responsibilities.

It can be seen from formulas (4)-(6) that when expected ramping output is used as the smallest quantified unit of responsibility: (a) The power-capacity $P_{K,max}$ can also be regarded as storage resources in addition to water resources in Category 2) unreliable factors. That is, the storage resources include unit resources and primary energy resources. (b) The objective factor of the component itself in Category 1) unreliable factors include the failure of units and the power drop of wind power.

3. TRACING MODEL BASED ON TEMPORAL RECURSION

3.1. Decomposition of load shedding

From formula (3), it can be seen that E^t is composed of two parts, which are E^{t-1} and $R'_D - R^t$. Therefore, in chronological order, E^t is decomposed into 2 parts, denoted by formula (8)-(9), as shown in Step1 in Figure 2.

$$E'_1 = \min(E^t, E^{t-1}) \quad (8)$$

$$E'_2 = E^t - E'_1 \quad (9)$$

As for E'_1 , the same as reference [21], it is also allocated to each component according to the known allocation ratio $e^{t-1}=[e_1^{t-1}, e_2^{t-1}, \dots, e_k^{t-1}, \dots, e_n^{t-1}]^T$. k is also the serial number of components, and it refers to the component number to which the load shedding is finally allocated.

As for E'_2 , it is the load shedding corresponding to $R'_D - R^t$. The magnitude by which the actual supply is smaller than the expected value is called the expected ramping insufficiency, denoted by formula (10). And E'_2 is temporarily allocated to components in period $(t-1,t)$ according to the proportion of expected ramping insufficiency, as shown in Step 2 in Figure 2. The amount of E'_2 temporarily allocated to component K in period $(t-1,t)$ is denoted by formula (11).

$$\Delta R'_{K,insu} = \max(0, R'_{K,D} - R'_K), K = 1, 2, \dots, n \quad (10)$$

$$E'_{K,2} = E'_2 \times \Delta R'_{K,insu} / \sum_{K=1}^n \Delta R'_{K,insu}, K = 1, 2, \dots, n \quad (11)$$

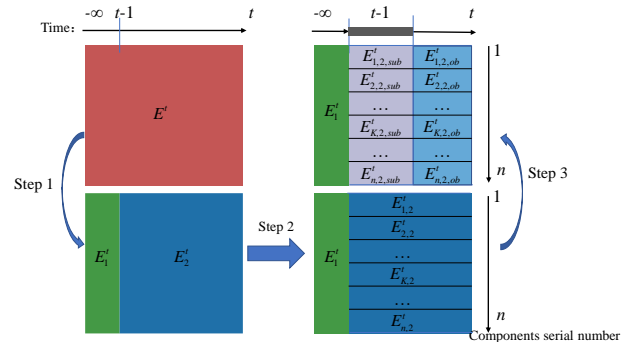


Figure 2 The decomposition of the amount of load shedding

As for $\Delta R'_{K,insu}$, it may be caused by the two categories of unreliable factors analyzed in Section 2 simultaneously. For

example, there may be situations where the storage water of a hydropower station is insufficient, and the hydropower unit fails at the same time. For the sake of simplicity, this paper decomposes $\Delta R_{K,insu}^t$ into 2 parts, denoted by formula (12)-(13).

$$\Delta R_{K,sub}^t = \max(0, R_{K,D}^t - R_{K,M}^t) \quad (12)$$

$$\Delta R_{K,ob}^t = \Delta R_{K,insu}^t - \Delta R_{K,sub}^t \quad (13)$$

Where $R_{K,M}^t$ is the ramping capacity of component K when component K does not fail, denoted by formula (14). $R_{K,Mprimary}^t$ is the ramping capacity of the hydropower limited by the primary energy, and $R_{K,Munit}^t$ is the ramping capacity of the hydropower limited by the unit resources.

$$R_{K,M}^t = \begin{cases} \min(r_K \Delta t, P_{K,max} - P_K^{t-1}), & K \in \Phi \\ \min(R_{K,Mprimary}^t, R_{K,Munit}^t), & K \in \Psi \end{cases} \quad (14)$$

$$R_{K,Mprimary}^t = (V_K^{t-1} + I_K^t - V_{K,min}) A_K H_K / \Delta t - P_K^{t-1}, \quad K \in \Psi \quad (15)$$

$$R_{K,Munit}^t = P_{K,max} - P_K^{t-1}, \quad K \in \Psi \quad (16)$$

$\Delta R_{K,sub}^t$ is the part caused by insufficient ramping capacity at time $t-1$ due to Category 2) unreliable factors. $\Delta R_{K,ob}^t$ is the part aggravated by Category 1) unreliable factors in period $(t-1, t)$. And $E_{K,2}^t$ is also decomposed into 2 parts according to the proportion of $\Delta R_{K,sub}^t$ and $\Delta R_{K,ob}^t$, denoted by formula (17)-(18), as shown in Step 3 in Figure 2.

$$E_{K,2,sub}^t = E_{K,2}^t \times \Delta R_{K,sub}^t / \Delta R_{K,insu}^t \quad (17)$$

$$E_{K,2,ob}^t = E_{K,2}^t \times \Delta R_{K,ob}^t / \Delta R_{K,insu}^t \quad (18)$$

As for $\Delta R_{K,ob}^t$ or $E_{K,2,ob}^t$, the responsibility is allocated to component K itself. As for $\Delta R_{K,sub}^t$ or $E_{K,2,sub}^t$ caused by insufficient ramping capacity, it is necessary to trace back the components that caused unreliable factors in the pre-sequence period based on a retrospective allocation model. However, for the insufficient ramping capacity caused by Category 2) unreliable factors, the storage resources limiting ramping capacity include the unit and primary energy. The characteristics of these two types of resources are different. When tracing back to the components before time $t-1$, it is necessary to distinguish the characteristics of different limited storage resources. Therefore, this paper establishes different retrospective allocation models for different limited storage resources as shown in Section 3.2 and 3.3.

For thermal units, the primary energy is enough, and the ramping capacity is only limited by unit resources. So when the ramping capacity of the thermal unit is insufficient, $\Delta R_{K,sub}^t$ needs to be traced back according to the model in Section 3.2. For hydropower stations, the ramping capacity is limited by unit and primary energy at the same time. For the sake of simplicity: if $R_{K,Munit}^t < R_{K,Mprimary}^t$, $\Delta R_{K,sub}^t$ is traced back according to the model in Section 3.2; otherwise, $\Delta R_{K,sub}^t$ is traced back according to the model in Section 3.3.

3.2. Retrospective allocation model when the limited storage resources are unit resources

In the case of known initial power output and expected ramping at each time, the corresponding expected power output at each time is also known. The expected power output of component K at time $t-1$ is denoted by $P_{K,D}^{t-1}$. And the magnitude by which P_K^{t-1} is larger than $P_{K,D}^{t-1}$ is called expected power excess, denoted by formula (19).

$$\Delta P_{K,excess}^{t-1} = \max(0, P_K^{t-1} - P_{K,D}^{t-1}), \quad K = 1, 2, \dots, n \quad (19)$$

$$\Delta R_{K,excess}^t = \max(0, R_K^t - R_{K,D}^t), \quad K = 1, 2, \dots, n \quad (20)$$

It can be seen from formula (14) that the reason for $\Delta R_{K,sub}^t$ in terms of unit resources is that $\Delta P_{K,excess}^{t-1} > 0$. The reason for $\Delta P_{K,excess}^{t-1}$ is the cumulative effect of multiple excessive ramping of component K before time $t-1$, which aims to make up for the expected ramping insufficiency of other components. The magnitude by which the actual ramping supply is larger than the expected ramping value is called the expected ramping excess, denoted by formula (20).

Therefore, as shown in Figure 3, the first step of tracing the responsibility of $\Delta R_{K,sub}^t$ is: Decompose $\Delta R_{K,sub}^t$ into multiple parts respectively caused by $\Delta R_{K,excess}^{t_p}$, $t_p = f_p(t-1), \dots, t-1$. The proportion is denoted by formula (21).

$$a_K^{t_p} = \frac{\Delta R_{K,excess}^{t_p}}{\sum_{i=f_p(t-1)}^{t-1} \Delta R_{K,excess}^i}, \quad t_p = f_p(t-1), \dots, t-1 \quad (21)$$

Where $f_p(t-1)$ is the traceback front-end time when tracing unreliable factors that lead to expected power excess. In this paper, $f_p(t-1)$ is the time when $\Delta P_{K,excess}^{f_p(t-1)} > 0$ and $\Delta P_{K,excess}^{f_p(t-1)-1} = 0$ looking back from time $t-1$ for the first time. That is, for the sake of simplicity, this paper only considers the recent responsibility of the components that generated less power.

The reason for $\Delta R_{K,excess}^{t_p}$ is that there is load shedding at time t_p-1 and the ramping supply of components other than component K is too low at time t_p . Namely $E^{t_p-1} > 0$ and $\Delta R_{w,insu}^{t_p} > 0$, $w=1, \dots, K-1, K+1, \dots, n$. Among them, $E^{t_p-1} > 0$ will cause the system to shed load at time t_p , even if all components meet the expected ramping at time t_p . And $\Delta R_{w,insu}^{t_p} > 0$ will also cause the system to shed load at time t_p , if the components other than component w only meet the expected ramping value at time t_p . That is, in order to reduce the load shedding at time t_p , the $\Delta R_{K,excess}^{t_p}$ is caused. The above analysis is the same for $t_p = f_p(t-1), \dots, t-1$.

Therefore, $\Delta R_{K,sub}^t$ is caused by the following unreliable factors when the limited resources are unit resources:

$$\begin{bmatrix} E^{f_p(t-1)-1} & \dots & E^{t_p-1} & \dots & E^{t-2} \\ \Delta R_{1,insu}^{f_p(t-1)} & \dots & \Delta R_{1,insu}^{t_p} & \dots & \Delta R_{1,insu}^{t-1} \\ \Delta R_{2,insu}^{f_p(t-1)} & \dots & \Delta R_{2,insu}^{t_p} & \dots & \Delta R_{2,insu}^{t-1} \\ \vdots & \ddots & \vdots & \ddots & \vdots \\ \Delta R_{n,insu}^{f_p(t-1)} & \dots & \Delta R_{n,insu}^{t_p} & \dots & \Delta R_{n,insu}^{t-1} \end{bmatrix} \quad (22)$$

Then, as shown in Figure 3, the second step of tracing the responsibility of $\Delta R_{K,sub}^t$ is: Decompose $\Delta R_{K,sub}^t \times a_K^{t_p}$ into multiple parts respectively caused by E^{t_p-1} and $\Delta R_{w,insu}^{t_p}$, $w=1, \dots, K-1, K+1, \dots, n$. And repeat this process at $t_p = f_p(t-1), \dots, t-1$. Since $\Delta R_{K,insu}^{t_p} = 0$, the decomposition proportion at time t_p is denoted by formula (23) for simplicity of writing.

$$b_m^{t_p} = \begin{cases} E^{t_p-1} / (E^{t_p-1} + \sum_{w=1}^n \Delta R_{w,insu}^{t_p}), & m = 1 \\ \Delta R_{m-1,insu}^{t_p} / (E^{t_p-1} + \sum_{w=1}^n \Delta R_{w,insu}^{t_p}), & m = 2, \dots, n+1 \end{cases} \quad (23)$$

Repeating formula (23) at $t_p = f_p(t-1), \dots, t-1$, and combining it with formula (21), then the proportion of responsibility for causing $\Delta R_{K,sub}^t$ borne by the unreliable factors denoted by formula (22) is:

$$\begin{bmatrix} b_1^{f_p(t-1)} a_K^{f_p(t-1)} & \dots & b_1^{t_p} a_K^{t_p} & \dots & b_1^{t-1} a_K^{t-1} \\ \vdots & \ddots & \vdots & \ddots & \vdots \\ b_m^{f_p(t-1)} a_K^{f_p(t-1)} & \dots & b_m^{t_p} a_K^{t_p} & \dots & b_m^{t-1} a_K^{t-1} \\ \vdots & \ddots & \vdots & \ddots & \vdots \\ b_{n+1}^{f_p(t-1)} a_K^{f_p(t-1)} & \dots & b_{n+1}^{t_p} a_K^{t_p} & \dots & b_{n+1}^{t-1} a_K^{t-1} \end{bmatrix} \quad (24)$$

E^{t_p-1} and $\Delta R_{w,insu}^{t_p}$, $w=1,2,\dots,n$, $t_p=f_p(t-1),\dots,t-1$, in formula (22) have all been allocated to each component. As for E^{t_p-1} , the known allocation ratio is $\mathbf{e}^{t_p-1}=[e_1^{t_p-1},\dots,e_k^{t_p-1},\dots,e_n^{t_p-1}]^T$. As for $\Delta R_{w,insu}^{t_p}$, the known allocation ratio is $\mathbf{d}^{t_p}=[d_{1,w}^{t_p},\dots,d_{k,w}^{t_p},\dots,d_{n,w}^{t_p}]^T$. This is because the temporal recursive idea of this paper is updating the allocation ratio at time t based on the known allocation ratio before time t and using it for the calculation of the allocation ratio after time t .

Finally, the proportion of responsibility of $\Delta R_{K,sub}^t$ allocated to each component when the limited resources are unit resources is denoted by formula (25).

$$\begin{aligned} \mathbf{c}_K^{t-1} &= [c_{1,K}^{t-1} \quad \dots \quad c_{k,K}^{t-1} \quad \dots \quad c_{n,K}^{t-1}]^T \\ &= \sum_{t_p=f_p(t-1)}^{t-1} (b_1^{t_p} a_K^{t_p} \times \mathbf{e}^{t_p-1} + \sum_{m=2}^{n+1} b_m^{t_p} a_K^{t_p} \times \mathbf{d}_{m-1}^{t_p}) \end{aligned} \quad (25)$$

To sum up, the tracing back process of $\Delta R_{K,sub}^t$ when the limited resources are unit resources is illustrated in Table 1. Table 1 The tracing back process when the limited resources is unit resources

Algorithm	The tracing back process of $\Delta R_{K,sub}^t$ when the limited resources are unit resources
1	Initialize $\mathbf{c}_K^1=[0,0,\dots]^T$
2	Calculate the end time of the traceback, $f_p(t-1)$
3	Calculate a_K^t , $t_p=f_p(t-1),\dots,t-1$, according to formula (21)
4	for $t_p=t-1,t-2,\dots,f_p(t-1)$
5	Calculate $b_m^{t_p}, m=1,\dots,n+1$, according to formula (23)
6	$\mathbf{c}_K^{t+1} = \mathbf{c}_K^{t+1} + b_1^{t_p} a_K^{t_p} \times \mathbf{e}^{t_p-1} + \sum_{m=2}^{n+1} b_m^{t_p} a_K^{t_p} \times \mathbf{d}_{m-1}^{t_p}$
7	end for
Output	\mathbf{c}_K^{t-1}

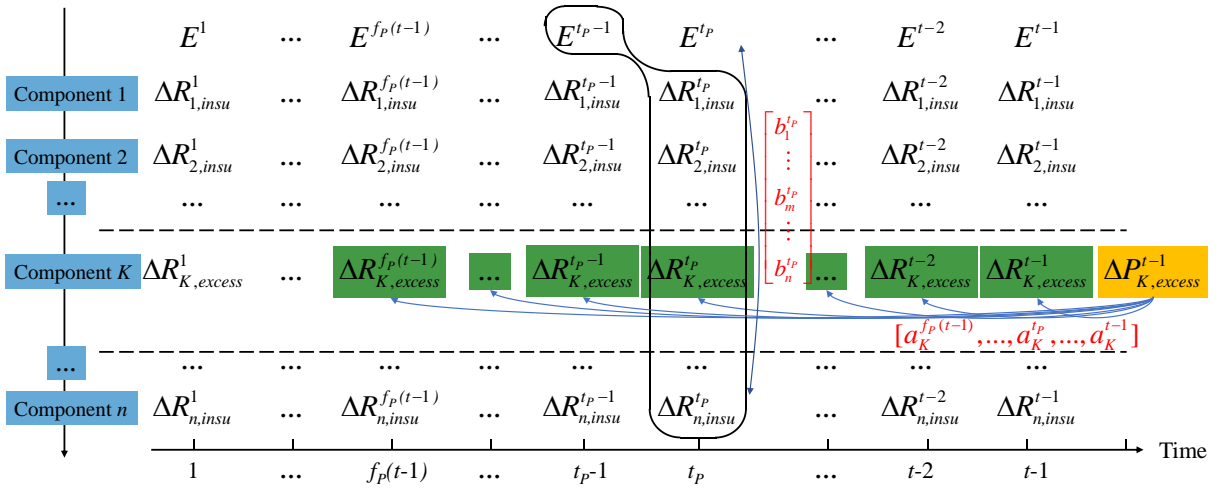


Figure 3 The tracing process of limited unit resources

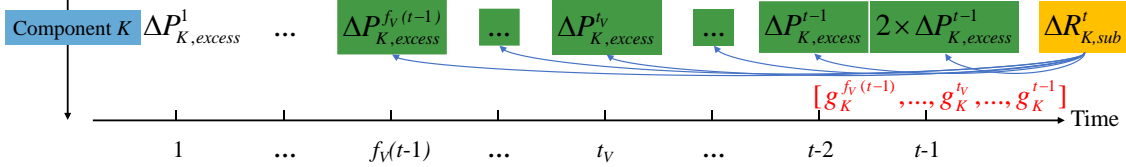


Figure 4 The tracing process of limited primary energy resources

3.3. Retrospective allocation model when the limited storage resources are primary energy resources

The reason for the shortage of water resources in hydropower station K is that component K continued to generate excessive power in the previous period. As shown in Figure 5(a), component K is scheduled to ramp $\Delta R_{K,excess}^{t-2}$ and $\Delta R_{K,excess}^{t-1}$ more than the expected value in period $(t-3,t-2)$ and $(t-2,t-1)$ respectively, in order to make up for the expected ramping insufficiency of component k_1 and k_2 respectively. Then, component K continuous to overconsume $\Delta R_{K,excess}^{t-2} \times 3\Delta t$ water resources in period $(t-3,t)$ due to the continuous low output of component k_1 , and continuous to overconsume $\Delta R_{K,excess}^{t-1} \times 2\Delta t$ water resources in period $(t-2,t)$ due to the continuous low output of component k_2 . If the overconsumption of these water resources leads to load shedding at time t , then the responsibility ratio that component k_1 needs to bear is $3\Delta R_{K,excess}^{t-2} / (3\Delta R_{K,excess}^{t-2} + 2\Delta R_{K,excess}^{t-1})$, and that component k_2 needs to bear is $2\Delta R_{K,excess}^{t-1} / (3\Delta R_{K,excess}^{t-2} + 2\Delta R_{K,excess}^{t-1})$.

$+2\Delta R_{K,excess}^{t-1}$.

The aforementioned allocation process is based on accumulating information through forward statistics. However, the expected ramping insufficiency of component k_1 and component k_2 may also be due to other unreliable factors before. Multiple and indeterminate numbers of nested loops may be required to allocate the responsibility for the load shedding to the fundamental unreliable factors. In order to allocate the responsibility based on the recursive model, this paper decomposes the total overconsumed water twice. The first decomposition of water resources overconsumed by component K , based on the expected ramping output as the smallest quantified unit of responsibility, is shown in Fig. 5(b)-(d).

As shown in Figure 5 (b)-(d), the total overconsumed water is firstly decomposed into 3 parts, namely Part 1, Part 2, and Part 3. Among them, the accumulated overconsumed water in period $(t-3,t-1)$, namely the sum of Part 1 and Part 2, can also be regarded as the magnitude of V_K^{t-1} smaller than $V_{K,D}^{t-1}$.

$V_{K,D}^{t-1}$ is the expected water volume of reservoir K at time $t-1$. The expected water volume of the reservoir at each time is known in the case of known initial power output and expected ramping at each time. And the magnitude by which V_K^{t-1} is smaller than $V_{K,D}^{t-1}$ is called the expected volume insufficiency, denoted by formula (26).

$$\Delta V_{K,insu}^{t-1} = \max(0, V_{K,D}^{t-1} - V_K^{t-1}), K=1,2,\dots,n \quad (26)$$

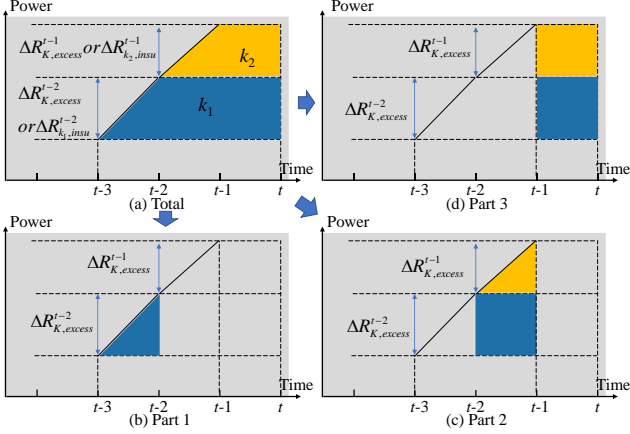


Figure 5 Decomposition of overconsumed water resources

The three parts of overconsumed water in Figure 5 can also be regarded as the expected power excess at time $t-2$, $t-1$, and t multiplied by Δt . And the excessive power output is the integral effect of the expected ramping excess. For example, Part 3 is caused by the excess output of component K by the size of $\Delta R_{K,excess}^{t-2} + \Delta R_{K,excess}^{t-1}$ in period $(t-1, t)$. Therefore, the second decomposition is to decompose the excessive power output multiplied by Δt into several parts caused by the expected ramping excess multiplied by Δt .

Similar to the two decompositions of the total overconsumed water, the two steps of tracing the responsibility of $\Delta R_{K,sub}^t$ are as follows:

Firstly, decompose $\Delta R_{K,sub}^t$ into multiple parts respectively caused by $\Delta P_{K,excess}^{t_V}$, $t_V=f_V(t-1), \dots, t-1$, as shown in Figure 4. The proportion is denoted by formula (27).

$$g_K^{t_V} = \begin{cases} \frac{\Delta P_{K,excess}^{t_V}}{\sum_{i=f_V(t-1)}^{t-1} \Delta P_{K,excess}^i + \Delta P_{K,excess}^{t-1}}, t_V = f_V(t-1), \dots, t-2 \\ \frac{2 \times \Delta P_{K,excess}^{t-1}}{\sum_{i=f_V(t-1)}^{t-1} \Delta P_{K,excess}^i + \Delta P_{K,excess}^{t-1}}, t_V = t-1 \end{cases} \quad (27)$$

$$\mathbf{d}_K^t = \begin{bmatrix} d_{1,K}^t \\ \vdots \\ d_{K-1,K}^t \\ d_{K,K}^t \\ d_{K+1,K}^t \\ \vdots \\ d_{n,K}^t \end{bmatrix} = \begin{cases} \frac{\Delta R_{K,sub}^t}{\Delta R_{K,insu}^t} \times [c_{1,K}^{t-1} \ \dots \ c_{K-1,K}^{t-1} \ c_{K,K}^{t-1} \ c_{K+1,K}^{t-1} \ \dots \ c_{n,K}^{t-1}]^T + \frac{\Delta R_{K,ob}^t}{\Delta R_{K,insu}^t} \times [0 \ \dots \ 0 \ 1 \ 0 \ \dots \ 0]^T \\ \quad , K \in \Phi \parallel (K \in \Psi \ \&\& R_{K,Mprimary}^t > R_{K,Munit}^t) \\ \frac{\Delta R_{K,sub}^t}{\Delta R_{K,insu}^t} \times [h_{1,K}^{t-1} \ \dots \ h_{K-1,K}^{t-1} \ h_{K,K}^{t-1} \ h_{K+1,K}^{t-1} \ \dots \ h_{n,K}^{t-1}]^T + \frac{\Delta R_{K,ob}^t}{\Delta R_{K,insu}^t} \times [0 \ \dots \ 0 \ 1 \ 0 \ \dots \ 0]^T \\ \quad , K \in \Psi \ \&\& R_{K,Mprimary}^t \leq R_{K,Munit}^t \\ \frac{\Delta R_{K,ob}^t}{\Delta R_{K,insu}^t} \times [0 \ \dots \ 0 \ 1 \ 0 \ \dots \ 0]^T, K \in \Omega \end{cases} \quad (31)$$

Where $f_V(t-1)$ is the traceback front-end time when tracing unreliable factors that lead to insufficient primary energy resources. In this paper, $f_V(t-1)$ is the time when $\Delta V_{K,insu}^{f_V(t-1)-1} = 0$ && $\Delta P_{K,excess}^{f_V(t-1)-1} = 0$ && ($\Delta V_{K,insu}^{f_V(t-1)} > 0$ or $\Delta P_{K,excess}^{f_V(t-1)} > 0$) looking back from time $t-1$ for the first time.

In formula (27), the impact of the expected power excess at time $t-1$ is doubled. This is because the overconsumed water of Part 2 and Part 3 in Figure 5 are the same size when the area of the triangle is approximately the same as the rectangle, which can all be considered as the expected power excess at time $t-1$ multiplied by Δt .

Secondly, as described in Section 3.2, $\Delta P_{K,excess}^{t_V}$ is caused by the unreliable factors denoted by formula (28). And the proportion of responsibility allocated to each component for causing $\Delta P_{K,excess}^{t_V}$ is denoted by formula (29), which is the same as formula (25).

$$\begin{bmatrix} E^{f_V(t_V)-1} & \dots & E^{t_V-1} & \dots & E^{t_V-1} \\ \Delta R_{1,insu}^{f_V(t_V)} & \dots & \Delta R_{1,insu}^{t_V} & \dots & \Delta R_{1,insu}^{t_V} \\ \Delta R_{2,insu}^{f_V(t_V)} & \dots & \Delta R_{2,insu}^{t_V} & \dots & \Delta R_{2,insu}^{t_V} \\ \vdots & \ddots & \vdots & \ddots & \vdots \\ \Delta R_{n,insu}^{f_V(t_V)} & \dots & \Delta R_{n,insu}^{t_V} & \dots & \Delta R_{n,insu}^{t_V} \end{bmatrix} \quad (28)$$

$$\begin{aligned} \mathbf{c}_K^{t_V} &= [c_{1,K}^{t_V} \ \dots \ c_{k,K}^{t_V} \ \dots \ c_{n,K}^{t_V}]^T \\ &= \sum_{t_p=f_V(t_V)}^{t_V} (b_1^{t_p} a_K^{t_p} \times \mathbf{e}^{t_p-1} + \sum_{m=2}^{n+1} b_m^{t_p} a_K^{t_p} \times \mathbf{d}_{m-1}^{t_p}) \end{aligned} \quad (29)$$

The above unreliable factors analysis and allocation ratio are the same for $t_V=f_V(t-1), \dots, t-1$. Therefore, the proportion of responsibility of $\Delta R_{K,sub}^t$ allocated to each component when the limited resources are primary energy resources is:

$$\mathbf{h}_K^{t-1} = [h_{1,K}^{t-1} \ \dots \ h_{k,K}^{t-1} \ \dots \ h_{n,K}^{t-1}]^T = \sum_{t_V=f_V(t-1)}^{t-1} g_K^{t_V} \mathbf{c}_K^{t_V} \quad (30)$$

To sum up, the tracing back process of $\Delta R_{K,sub}^t$ when the limited resources are primary energy resources is illustrated in Table 2.

Table 2 The tracing back process when the primary energy resources is unit resources

Algorithm II	The tracing back process of $\Delta R_{K,sub}^t$ when the limited resources are primary energy resources
1	Initialize $\mathbf{h}_K^{t-1} = [0, \dots, 0]^T$
2	Calculate the end time of the traceback, $f_V(t-1)$
3	Calculate $g_K^{t_V}$, $t_V=f_V(t-1), \dots, t-1$, according to formula (27)
4	for $t_V=t-1, t-2, \dots, f_V(t-1)$
5	Calculate $\mathbf{c}_K^{t_V}$ according to Algorithm I
6	$\mathbf{h}_K^{t-1} = \mathbf{h}_K^{t-1} + g_K^{t_V} \mathbf{c}_K^{t_V}$
7	end for
Output	\mathbf{h}_K^{t-1}

3.4. Update of the allocation ratio

Section 3.2 and 3.3 analyze the tracing process of $\Delta R_{k,sub}^t$ in different situations. Combined with $\Delta R_{k,ob}^t$ in Section 3.1, the update of $\mathbf{d}_k^t=[d_{1,k}^t, \dots, d_{k,k}^t, \dots, d_{n,k}^t]^T$ is shown in formula (31). In formula (31), the update of \mathbf{d}_k^t is divided into three situations according to the properties and parameters of component K . Situation 1: The limited resources are unit resources, that is, component K is thermal power, or component K is hydropower but the ramping capacity is limited due to unit resources. Situation 2: The limited resources are primary energy resources, that is, component K is hydropower and the ramping capacity is limited due to primary energy resources. Situation 3: Component K is wind power.

Repeat the above process for $K=1,2,\dots,n$. Eventually, the amount of E^t allocated to each component is shown in formula (32), and the update of $\mathbf{e}^t=[e_1^t, \dots, e_k^t, \dots, e_n^t]^T$ is shown in formula (33). The calculation of \mathbf{e}^t and \mathbf{d}_k^t requires their own value in the previous times, so this model is a temporal recursive process.

$$\mathbf{E}^t = [E_1^t \ \dots \ E_k^t \ \dots \ E_n^t]^T = E_1^t \times \mathbf{e}^{t-1} + \sum_{K=1}^n (E_{K,2}^t \times \mathbf{d}_K^t) \quad (32)$$

$$\mathbf{e}^t = \mathbf{E}^t / E^t \quad (33)$$

To sum up, the tracing process of E^t is illustrated in Table 3.

Table 3 The calculation flowchart for unreliability tracing

Input	The expected value of each component in period $(t-1, t)$ and time $t-1$, including $R_{k,D}^t, P_{k,D}^t, V_{k,D}^t$. The actual value of each component in period $(t-1, t)$ and at time $t-1$, including R_k^t, P_k^t, V_k^t . The known E^{t-1} . The known allocation ratio of each component before time t , including \mathbf{e}^t and $\mathbf{d}_k^t, t < t, K=1,2,\dots,n$.
1	Calculate E^t according to formula (3)
2	Calculate E_1^t and E_2^t according to formulas (8) and (9)
3	Calculate $E_{k,2}^t, K=1,2,\dots,n$, according to formula (11)
4	for $K=1,2,\dots,n$
5	Calculate $\Delta R_{k,sub}^t$ and $\Delta R_{k,ob}^t$ according to formulas (12) and (13)
6	if $K \in \Phi$ $(K \in \Psi \ \&\& \ R_{k,Mprimary}^t > R_{k,Munit}^t)$
7	Calculate \mathbf{c}_k^t according to Algorithm I
8	elseif $K \in \Psi$ && $R_{k,Mprimary}^t \leq R_{k,Munit}^t$
9	Calculate \mathbf{h}_k^t according to Algorithm II
10	endif
11	Calculate \mathbf{d}_k^t according to formula (31)
12	endfor
13	Calculate \mathbf{E}^t and \mathbf{e}^t according to formulas (32) and (33)
Output	$\mathbf{E}^t, \mathbf{e}^t$, and $\mathbf{d}_k^t, K=1,2,\dots,n$

Assuming that the reliability indices EENS (expected energy not supplied) are obtained by simulating T times, and the time interval between the two times is 1 hour, that is:

$$EENS = \sum_{t=1}^T E^t \times \frac{8760}{T} \quad (34)$$

Then, the reliability indices EDNS and EENS allocated to component k can be denoted by formula (35); and the allocated percentage is as shown in formula (36).

$$EENS_k = \sum_{t=1}^T E_k^t \times \frac{8760}{T}, k = 1, 2, \dots, n \quad (35)$$

$$EENS_k \% = \frac{EENS_k}{EENS} \times 100\%, k = 1, 2, \dots, n \quad (36)$$

4. CASES STUDY

This section describes the calculation process of the proposed tracing model and the rationality of the tracing

results based on systems of three scales.

1) A simple system with 3 components. The calculation process of the tracing model is explained based on a load-shedding event of this simple system.

2) Modified RBTS[22]. The rationality of the model proposed in this paper is proved, and the allocation result is compared with the results of the traditional tracing model.

3) Modified RTS[23]. The unreliability tracing of this system is performed to illustrate the applicability of the model within a large-scale power system.

4.1. A simple system

The component parameters are shown in Table 4 and Table 5. Where $V_{k,max}$ is the maximum water volume of reservoir k . Load, expected and actual values of power output, expected and actual values of ramping, and water volume of the components are shown in rows 2-8 of Table 6. Among them, the unit of component 2 fails in period (1,2), so the actual power output of component 2 is 0MW at time 2. Component 1 is wind power and the actual power output drops between time 3 and time 4.

Table 4 Parameters of components

Component no.	Component category	Rated power-capacity (MW)	Rated ramp rate (MW/h)
1	Wind	40	—
2	Thermal	40	10
3	Hydro	80	—

Table 5 Parameters of hydropower stations

Component no.	$V_{k,min}$ (10^5m^3)	$V_{k,max}$ (10^5m^3)	Natural inflow mean (m^3/s)	H_k (m)	A_k
3	20	70	0	100	8

Table 6 The expected and actual value of components

Index	Component no.	$t=1$	$t=2$	$t=3$	$t=4$
Load (MW)	System	80	80	90	90
	1	20	20	20	20
	2	20	20	25	25
$P_{k,D}$ (MW)	3	40	40	45	45
	1	—	0	0	0
	2	—	0	5	0
$R_{k,D}$ (MW)	3	—	0	5	0
	1	—	0	0	0
	2	—	0	5	0
$V_{k,D}$ (10^5m^3)	3	25.850	24.050	22.025	20
P_k (MW)	1	20	20	10	10
	2	20	0	10	20
	3	40	60	70	0
R_k (MW)	1	—	0	-10	0
	2	—	-20	10	10
	3	—	20	10	-70
V_k^t (10^5m^3)	3	25.850	23.150	20	20
E^t (MW)	System	0	0	0	60
	1	—	0	10	0
	2	—	20	0	0
	3	—	0	0	70
	3	0	20	25	0
$\Delta R_{k,insu}^t$ (MW)	3	—	20	5	0
	1	—	0	10	0
	2	—	20	0	0
$\Delta P_{k,excess}^t$ (MW)	3	0	20	25	0
	3	—	20	5	0

Then, as shown in row 9 of Table 6, there is load shedding at time 4, i.e., $E^4=60\text{MW}$. Partial data on the differences between the actual value and expected value are also shown in Table 6. The allocation process of E^4 is as follows:

1) $E_1^4=0\text{MW}, E_2^4=60\text{MW}$. Only $E_2^4=60\text{MW}$ needs to be allocated. According to the proportion of $\Delta R_{k,insu}^4, K=1,2,3$, the amount of E_2^4 allocated to each component in period (3,4) is $E_{1,2}^4=0\text{MW}, E_{2,2}^4=0\text{MW}, E_{3,2}^4=60\text{MW}$. That is, only

component 3 is allocated the responsibility if there is no further tracing.

2) $E_{3,2}^4$ or $\Delta R_{3,insu}^4$ are all due to Category 2) unreliable factors, and the limited storage resource is primary energy. According to $\Delta P_{3,excess}^t$ shown in Table 6, the calculation results of g_3^t are shown in Table 7. And according to $\Delta R_{3,excess}^t$ shown in Table 6, the calculation results of a_3^t for each time of $t_Y=2,3$, are also shown in Table 8.

3) According to $\Delta R_{K,insu}^t$ and E^{t-1} , $K=1,2,3$, $t=2,3$, shown in Table 6, the calculation results of b_m^2 and b_m^3 are shown in Table 9.

4) The unreliable factors causing $\Delta R_{2,insu}^2$ and $\Delta R_{1,insu}^3$ are the unit failure of component 2 and the power output drops of component 3 respectively. These are all Category 1) unreliable factors. That is, d_2^2 and d_1^3 are known and are shown in Table 10. Finally, the results of h_3^4 , d_3^4 , E^4 and e^4 are also shown in Table 10. After further tracing, the responsibility of E^4 is fully allocated to components 1 and 2. And these two components are the objective factors leading to load shedding.

Table 7 The calculation results of g_3^t

Index	$t_Y=1$	$t_Y=2$	$t_Y=3$
g_3^t	0	0.286	0.714

Table 8 The calculation results of a_3^t

Index	$t_P=2$	$t_P=3$
a_3^t ($t_Y=2$)	1	—
a_3^t ($t_Y=3$)	0.8	0.2

Table 9 The calculation results of b_m^2 and b_m^3

Variable m	b_m^2	b_m^3
System	0	0
Component 1	0	1
Component 2	1	0
Component 3	0	0

Table 10 The allocated proportion of components

Component no.	$d_{k,2}^2$	$d_{k,3}^2$	$h_{k,3}^4$	$d_{k,3}^4$	E_k^4 (MW)	e_k^4
1	0	1	0.143	0.143	8.571	0.143
2	1	0	0.857	0.857	51.429	0.857
3	0	0	0	0	0	0

4.2. Modified RBTS

4.2.1. System parameters

In this paper, 3 hydropower stations and 4 wind farms are added based on RBTS to form a modified RBTS. The load peak is 418MW, and the parameters are shown in Table 11-Table 13. Where the average downward power fluctuation in Table 13 is used to represent the fluctuation characteristics of wind power. The statistical period is the LOLE moment with the highest probability of load shedding.

Table 11 Unit parameters of thermal units and hydropower stations of the modified RBTS

Component no.	$P_{k,max}$ (MW)	Number of units	Forced outage rate	r_k (MW/h)
1(thermal 1)	10	1	0.0201	12
2(thermal 2)	20	1	0.025	15
3(thermal 3)	40	1	0.0299	24
4(thermal 4)	40	1	0.0299	60
5(thermal 5)	5	1	0.0102	10
6(thermal 6)	5	1	0.0102	10
7(thermal 7)	20	1	0.0148	30
8(thermal 8)	20	1	0.0148	30
9(thermal 9)	20	1	0.0148	15

10(thermal 10)	20	1	0.0148	15
11(thermal 11)	40	1	0.0201	24
12(hydro 1)	40	1	0.0246	—
13(hydro 2)	40	1	0.0294	—
14(hydro 3)	40	1	0.0388	—

Table 12 Parameters of hydropower stations of the modified RBTS

Component no.	$V_{k,max}$ (10^8m^3)	$V_{k,min}$ (10^8m^3)	Natural inflow mean (m^3/s)	H_k (m)	A_k
12-14(hydro 1-3)	1.186	0.426	24.182	100	8

Table 13 Parameters of wind farms of the modified RBTS

Component no.	$P_{k,max}$ (MW)	Average downward power fluctuation (MW/h)
15(wind 1)	50	-0.74
16(wind 2)	50	-0.58
17(wind 3)	50	-1.86
18(wind 4)	50	-2.71

Based on the above-modified RBTS, on the one hand, the rationality of the tracing model proposed in this paper is proved by comparing the component parameters and the improvement of system reliability after the improvement of the components. On the other hand, it is proved that the allocation result of the model proposed in this paper is more accurate compared with the results of the traditional tracing model.

4.2.2. Allocation results and improvement effect

The reliability evaluation results of the above-modified RBTS are: LOLE=85.14 hour/a, EENS=1544.43 MWh/a. Based on the tracing model proposed in this paper, EENS=1544.43 MWh/a is allocated to components. The allocated percentage of each component is shown in column 2 of Table 14, the results are analyzed as follows:

a) The allocated percentage of thermal unit 4 is larger than thermal unit 3. This is because the rated power-capacity and forced outage rate of thermal units 3 and 4 are the same, as well as the larger rated ramp rate for thermal unit 4. So thermal unit 4 is expected to have greater responsibility, and this will make it have a greater impact once the unit fails. Similarly, hydropower station 3 is allocated the largest responsibility among the hydropower stations. This is because the forced outage rate of hydropower station 3 is the largest, while other parameters are the same as the other hydropower stations.

b) The rated power-capacity of each wind farm is the same, but the fluctuation parameters of each wind farm are different. It can be seen from Table 13 and Table 14 that the trend of the allocated percentage of wind farms is basically consistent with the trend of fluctuation parameters. Of course, it is not possible to judge the responsibility allocated to wind farms solely by this indicator, because the size and weight of the load shedding at different times are different. The statistics indicators here are just a simple explanation of the possible reasons.

In addition, in order to further verify the rationality of the model in this paper, improvements were made to individual components, simulating enhanced system reliability through maintenance measures and other measures. The methods of improvement for thermal units and wind farms differ. For thermal units and hydropower stations, their forced outage rates were reduced to 50% of the previous levels, respectively. For each wind farm, the downward fluctuation amplitude of wind power was decreased to 80% of its previous magnitude by incorporating energy storage.

Then the EENS of the respectively improved systems are shown in column 3 of Table 14, and the decrease in EENS relative to the initial system are shown in column 4 of Table 14. The results are analyzed as follows:

a) Because the fundamental unreliable factors of thermal power and hydropower are unit failures, the improvement of these two types of components can be uniformly quantified. Figure 6(a) shows the allocated percentage of thermal units and hydropower stations, and Figure 6(b) shows the EENS decrease after improving thermal units and hydropower stations. From Figure 6, it can be seen that the trend of the allocated percentage of hydropower stations and thermal units is basically consistent with the trend of improvement.

b) Since the improvement methods of the unit and the wind farm are different, it is necessary to compare wind farms separately. It can be seen from Table 14 that the trend of the allocated percentage of each wind farm is also consistent with the trend of improvement of system reliability.

Based on the results in Table 14, it is evident that choosing thermal unit 4 is preferable for reducing unit failure rates, while opting for wind farm 4 is recommended for reducing the fluctuation of wind power. The reduction in system load shedding risk is more pronounced in comparison to enhancing other components.

Table 14 EENS allocation results and improvement of system reliability in the modified RBTS

Component no.	Allocated percentage (%) - Proposed model	EENS of the improved system (MWh/a)	EENS decrease of the improved system (MWh/a)	Allocated percentage (%) - Traditional model
1(thermal 1)	0.79	1531.56	12.87	0.93
2(thermal 2)	2.48	1506.38	38.05	2.64
3(thermal 3)	9.61	1401.42	143.01	9.84
4(thermal 4)	12.31	1385.31	159.12	12.59
5(thermal 5)	0.15	1541.94	2.49	0.26
6(thermal 6)	0.18	1541.86	2.57	0.28
7(thermal 7)	1.63	1522.71	21.72	1.98
8(thermal 8)	1.95	1522.53	21.90	2.29
9(thermal 9)	1.36	1528.85	15.58	1.61
10(thermal 10)	1.40	1521.60	22.84	1.7
11(thermal 11)	8.36	1431.58	112.85	8.42
12(hydro 1)	7.20	1467.86	76.57	8.66
13(hydro 2)	9.50	1415.77	128.66	10.94
14(hydro 3)	11.24	1401.06	143.37	12.49
15(wind 1)	4.20	1538.29	6.14	3.21
16(wind 2)	3.92	1539.54	4.89	3.11
17(wind 3)	9.00	1537.00	7.43	6.8
18(wind 4)	14.73	1533.30	11.13	12.24
System	100.00	—	—	100.00

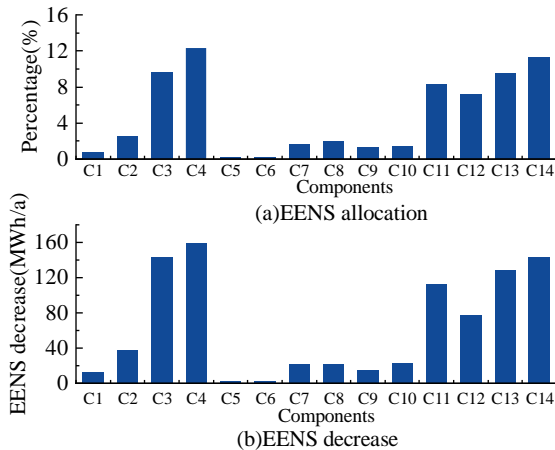


Figure 6 The allocation results and the improvement of system reliability after improving thermal units and hydropower stations respectively in the

modified RBTS

4.2.3. Comparison with traditional tracing models

This section compares the tracing model proposed in this paper with the traditional model. The traditional model refers to the model without further tracing to the previous time proposed in reference [21].

As for the modified RBTS in Section 4.2.1. The allocation results of EENS=1544.43 MWh/a based on the traditional tracing model are shown in column 5 of Table 14. And Table 15 counts the total allocated percentage of the three types of power sources. From Table 15, it can be seen that the responsibility allocated to all wind farms is larger in the proposed model compared with the traditional tracing model, and the responsibility allocated to all hydropower stations and all thermal units are smaller. That is, part of the responsibility allocated to hydropower and thermal power in the traditional model is traced back to wind power in the proposed model.

In order to illustrate that the allocation results in this paper are more accurate, this paper compares two cases: in case 1, thermal units 3, 4, and 11 are improved at the same time; and in case 2, hydropower stations 1-3 are improved at the same time. In these two cases, the improvement methods are both to reduce the forced outage rate of the 3 units to 50% of the previous. The EENS and decrease in EENS relative to the initial system in the two cases are shown in Table 16. And the total allocated percentages of the 3 components in the two cases in the proposed tracing model and in the traditional tracing model are also shown in Table 16. It can also be seen that the EENS decrease is 389.14 MWh/a in case 1, which is larger than 335.39 MWh/a in case 2. This is consistent with the allocation results of the model proposed in this paper and is not consistent with the allocation results of the traditional model. Therefore, the allocation results of the tracing model proposed in this paper are more reasonable and accurate compared with the traditional model.

Table 15 The total allocated percentage of the three types of power sources in the modified RBTS (unit: %)

Component no.	Traditional model	Proposed model
1-11(thermal 1-11)	42.54	40.21
12-14(hydro 1-3)	32.10	27.95
15-18(wind 1-4)	25.36	31.84

Table 16 The allocation results and improvement effect in two cases in the modified RBTS (unit: %)

Case no.	EENS of the improved system (MWh/a)	EENS decrease of the improved system (MWh/a)	Allocated percentage (%) - Proposed model	Allocated percentage (%) - Traditional model
1	1155.29	389.14	30.28	30.85
2	1209.04	335.39	27.95	32.1

4.3. Modified RTS

In this section, 6 hydropower stations and 9 wind farms are added based on RTS to form a modified RBTS. The partial parameters are shown in Table 17-Table 18, and the load peak is 5850MW. The reliability evaluation results are: LOLE=78.58 hour/a, EENS=19876.59 MWh/a. And EENS=19876.59 MWh/a is allocated to components.

Table 17 Partial parameters of the modified RTS

Component no.	$P_{k,max}$ (MW)	Number of units	Forced outage rate	r_k (MW/h)
1-5 (thermal 1-5)	12	5	0.0200	60
6-9(thermal 6-9)	20	4	0.1000	50
10-15(thermal 10-15)	50	6	0.0100	60
16-19(thermal 16-19)	76	4	0.0200	120
20-22(thermal 20-22)	100	3	0.0400	80
23-26(thermal 23-26)	155	4	0.0400	100
27-29(thermal 27-29)	197	3	0.0500	100
30(thermal 30)	350	1	0.0800	120
31-32(thermal 31-32)	400	2	0.1200	140
33(hydro 1)	270	1	0.0100	—
34(hydro 2)	270	1	0.0100	—
35(hydro 3)	270	1	0.0200	—
36(hydro 4)	270	1	0.0200	—
37(hydro 5)	270	1	0.0400	—
38(hydro 6)	270	1	0.0400	—
39-42(wind 1-4)	200	4	—	—
43-45(wind 5-7)	300	3	—	—
46-47(wind 8-9)	400	2	—	—

Table 18 Parameters of hydropower stations of the modified RTS

Component no.	$V_{k,max}$ (10^8m^3)	$V_{k,min}$ (10^8m^3)	Natural inflow mean (m^3/s)	H_k (m)	A_k
33-38(hydro 1-6)	5.5	3.1	163.23	100	8

Similarly to Section 4.2, it can also be seen that: 1) As shown in Figure 7, the trend of the allocated percentage of wind farms is basically consistent with the trend of fluctuation parameters. 2) Improve thermal units 20, 24-26, and 29-30 at the same time in case 1, and improve hydropower stations 1-6 at the same time in case 2. Then, as shown in Table 19, it can also be seen that the EENS decrease is 4828.76 MWh/a in case 1, which is larger than 2228.34 MWh/a in case 2. This is consistent with the allocation results of the model proposed in this paper and is not consistent with the allocation results of the traditional model.

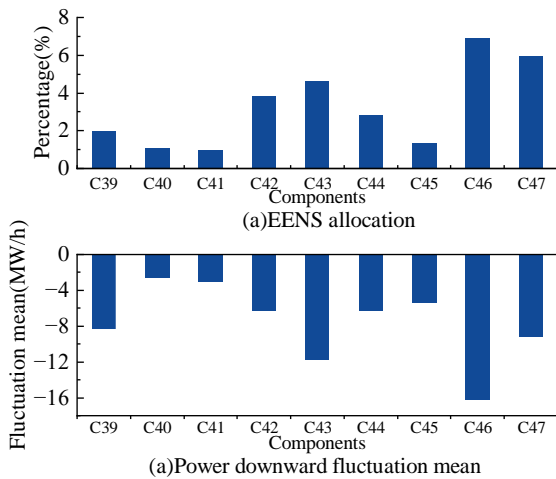


Figure 7 The allocation results and average downward power fluctuation of wind farms in the modified RTS

Table 19 The allocation results and improvement effect in two cases in the modified RTS (unit: %)

Case no.	EENS of improved systems (MWh/a)	EENS of decrease of improved systems (MWh/a)	Allocated percentage (%)- Proposed model	Allocated percentage (%)- Traditional model
1	15047.83	4828.76	17.80	17.05
2	17648.25	2228.34	7.33	17.30

5. CONCLUSION

This paper has presented an unreliability tracing model of power systems with hydropower. Several systems have been used for the case study. Simulation results have demonstrated the following findings:

1) Based on the temporal recursion, the unreliability tracing model proposed in this paper can realize the unified quantitative allocation of load shedding considering the primary energy shortage of hydropower stations equipped with a reservoir. It can realize the unified quantitative allocation of load shedding, considering wind power fluctuation, wind power intermittence, unit failures, and insufficient water storage.

2) The tracing model presented in this paper is reasonable. The trend of allocated percentage is basically consistent with the trend of component parameters and the improvement of system reliability with the same improvement to the components respectively.

3) The allocation results of the tracing model proposed in this paper are more reasonable compared with the traditional model. Thus, the weak components identified based on the tracing model proposed in this paper will also be more accurate than the traditional model.

6. ACKNOWLEDGMENTS

This work was supported by the National Natural Science Foundation of China under Grants 52022016.

7. REFERENCES

- IRENA: ‘Renewable capacity statistics 2023’ (The International Renewable Energy Agency, 2023) [Online]. Available: <https://www.irena.org/Publications/2023/Mar/Renewable-capacity-statistics-2023>
- Pourmoosavi, M.-A., Amraee, T.: ‘Low-carbon generation expansion planning considering flexibility requirements for hosting wind energy’ *IET Generation, Transmission & Distribution*, 2022, **16**, (16), pp. 3153–3170.
- Liu, Z., Hou, K., Jia, H., *et al.*: ‘A Lagrange Multiplier Based State Enumeration Reliability Assessment for Power Systems With Multiple Types of Loads and Renewable Generations’ *IEEE Transactions on Power Systems*, 2021, **36**, (4), pp. 3260–3270.
- Magness, B.: ‘Review of February 2021 Extreme Cold Weather Event – ERCOT Presentation’ (ERCOT, 2021) [Online]. Available: https://www.ercot.com/files/docs/2021/02/24/2.2_REVISIED_ERCOT_Presentation.pdf
- Palmintier, B.S., Webster, M.D.: ‘Impact of Operational Flexibility on Electricity Generation Planning With Renewable and Carbon Targets’ *IEEE Transactions on Sustainable Energy*, 2016, **7**, (2), pp. 672–684.
- Makarov, Y.V., Loutan, C., Ma, J., de Mello, P.: ‘Operational Impacts of Wind Generation on California Power Systems’ *IEEE Transactions on Power Systems*, 2009, **24**, (2), pp. 1039–1050.
- Karki, R., Hu, P., Billinton, R.: ‘Reliability Evaluation Considering Wind and Hydro Power Coordination’ *IEEE Transactions on Power Systems*, 2010, **25**, (2), pp. 685–693.
- Su, C., Cheng, C., Wang, P., Shen, J.: ‘Optimization Model for the Short-Term Operation of Hydropower Plants Transmitting Power to Multiple Power Grids via HVDC Transmission Lines’ *IEEE Access*,

- 2019, 7, pp. 139236–139248.
- 9 BP: ‘Statistical Review of World Energy 2022’ (bp, 2022) [Online]. Available: <https://www.bp.com/content/dam/bp/business-sites/en/global/corporate/pdfs/energy-economics/statistical-review/bp-stats-review-2022-full-report.pdf>
 - 10 Hou, W., Wei, H., Zhu, R.: ‘Data-driven multi-time scale robust scheduling framework of hydrothermal power system considering cascade hydropower station and wind penetration’ *IET Generation, Transmission & Distribution*, 2019, **13**, (6), pp. 896–904.
 - 11 Shi, X., Jia, R., Huang, Q., *et al.*: ‘Day-ahead complementary operation for wind-hydro-thermal system considering the multi-dimensional uncertainty’ *CSEE Journal of Power and Energy Systems*, 2022, pp. 1–11.
 - 12 Liu, B., Lund, J.R., Liao, S., Jin, X., Liu, L., Cheng, C.: ‘Peak Shaving Model for Coordinated Hydro-Wind-Solar System Serving Local and Multiple Receiving Power Grids via HVDC Transmission Lines’ *IEEE Access*, 2020, **8**, pp. 60689–60703.
 - 13 Wang, Y., Liu, C., Shahidehpour, M., Guo, C.: ‘Critical Components for Maintenance Outage Scheduling Considering Weather Conditions and Common Mode Outages in Reconfigurable Distribution Systems’ *IEEE Transactions on Smart Grid*, 2016, **7**, (6), pp. 2807–2816.
 - 14 Pordanjani, I.R., Wang, Y., Xu, W.: ‘Identification of Critical Components for Voltage Stability Assessment Using Channel Components Transform’ *IEEE Transactions on Smart Grid*, 2013, **4**, (2), pp. 1122–1132.
 - 15 Bahrami, S., Rastegar, M.: ‘Security-based critical power distribution feeder identification: Application of fuzzy BWM-VIKOR and SECA’ *International Journal of Electrical Power & Energy Systems*, 2022, **134**, p. 107395.
 - 16 Fattaheian-Dehkordi, S., Fotuhi-Firuzabad, M., Ghorani, R.: ‘Transmission System Critical Component Identification Considering Full Substations Configuration and Protection Systems’ *IEEE Transactions on Power Systems*, 2018, **33**, (5), pp. 5365–5373.
 - 17 Bhuiyan, M.Z.A., Anders, G.J., Philhower, J., Du, S.: ‘Review of static risk-based security assessment in power system’ *IET Cyber-Physical Systems: Theory & Applications*, 2019, **4**, (3), pp. 233–239.
 - 18 Melo, A.C.G., Pereira, M.V.F.: ‘Sensitivity analysis of reliability indices with respect to equipment failure and repair rates’ *IEEE Transactions on Power Systems*, 1995, **10**, (2), pp. 1014–1021.
 - 19 Li, S., Ma, Y., Hua, Y., Chen, P.: ‘Reliability Equivalence and Sensitivity Analysis to UHVDC Systems Based on the Matrix Description of the F&D Method’ *IEEE Transactions on Power Delivery*, 2016, **31**, (2), pp. 456–464.
 - 20 Xie, K., Billinton, R.: ‘Tracing the unreliability and recognizing the major unreliability contribution of network components’ *Reliability Engineering & System Safety*, 2009, **94**, (5), pp. 927–931.
 - 21 Bai, Y., Xie, K., Shao, C., Hu, B., Yu, X., Hu, Y.: ‘Unreliability tracing of power systems with high penetration of wind power based on a temporal decomposition model’ *CSEE Journal of Power and Energy Systems*, 2023, pp. 1–14.
 - 22 Billinton, R., Kumar, S., Chowdhury, N., *et al.*: ‘A reliability test system for educational purposes-basic data’ *IEEE Transactions on Power Systems*, 1989, **4**, (3), pp. 1238–1244.
 - 23 Subcommittee, P.M.: ‘IEEE Reliability Test System’ *IEEE Transactions on Power Apparatus and Systems*, 1979, **PAS-98**, (6), pp. 2047–2054.